Theory of the phase diagrams of lyotropic nematic and lyotropic cholesteric systems

P. Tolédano* and A.M. Figueiredo Neto
Instituto de Física, Universidade de São Paulo, Caixa Postal 66318, 05389-970 São Paulo, São Paulo, Brazil

V. Lorman
Université de Picardie, 80.000 Amiens, France

B. Mettout
Laboratoire de Physique des Solides, Ecole Superieure de Physique et de Chimie Industrielles de la Ville de Paris, 10 rue Vauquelin, 75231, Paris Cedex, France

V. Dmitriev
Institute of Physics, Rostov State University, 344104 Rostov on Don, Russia
(Received 13 March 1995)

A theoretical model of the isotropic-to-nematic or isotropic-to-cholesteric transitions is proposed, which applies to biaxial micellar aggregates undergoing a change in their shape. The current isotropic–biaxial-nematic theoretical model needs to be completed by considering an additional noncritical order parameter that expresses the change in the form of the micelles and produces a topological metamorphosis of the standard effective two-component order-parameter diagrams. This transformation results in a drastic restructuring of the phase diagrams, which involves a symmetric folding of the phases and singularities. A nonzero trace is assumed for the second-rank-tensor nematic order parameter.

PACS number(s): 61.30.Gd, 64.70.−p

I. INTRODUCTION

The theoretical description of lyotropic mesophases [1], which are formed by amphiphilic molecules dissolved in water, must account for the change in shape of the molecular aggregates with temperature and concentration [2]. The influence of the shape modification of the molecular subunits on the equilibrium structures, and on the topology of the corresponding phase diagrams, is complex, and two main situations must be distinguished in this respect. (1) The shape of the molecular aggregates changes continuously with the external variables, i.e., the evolution in their form corresponds to a *homogeneous deformation.* In this case the resulting equilibrium structures are generally related by group-subgroup relationships, and the transition between the corresponding structures can be of second order. (2) The molecular aggregates undergo a discontinuous modification in their geometry, with a drastic reorganization of the aggregates. In this situation one has the formation of new structures which may not be group-subgroup related to the initial structures, across first-order transitions. This is, for example, the case of the transformations occurring between lamellar, hexagonal, and cubic lyotropic phases [3].

The two preceding situations are usually found in the same lyotropic system for a different range of values of the external parameters. An illustrative example is given by the phase diagrams reported for lyotropic nematic phases [4,5] and lyotropic cholesteric phases [6–8], in which one can find two distinct regions: for low concentrations of the molecular aggregates in water, and below the isotropic fluid phase, the form of the micellar aggregates is modified progressively, forming uniaxial and biaxial nematic phases (or their cholesteric analogs) separated by second-order transition lines. For larger concentrations and lower temperatures, hexagonal and lamellar phases are stabilized, which are separated from the nematic, or cholesteric, region by first-order transition lines [8].

Figure 1 shows a number of typical phase diagrams which have been disclosed in lyotropic nematic and lyotropic cholesteric systems. Figure 1(a) represents the specific features of a lyotropic nematic diagram, as it was reported by Yu and Saupe [4] in the lyotropic mixture of potassium laurate, decanol, and water (D_2O). Three distinct nematic phases are stabilized, two uniaxial (denoted N_D and N_C) and one biaxial (N_B), which merge at a four-phase "Landau point" with the high-temperature isotropic structure (Iso 1). Another reentrant isotropic phase (Iso 2) takes place at lower temperature. When potassium laurate is replaced by decyl ammonium chloride [5] the uniaxial nematic phases are exchanged with respect to their position in Fig. 1(a) and the Iso 2 phase is replaced by a hexagonal two-dimensional structure [Fig. 1(b)]. At high concentrations, one may have either a lamellar or a hexagonal phase depending on the

*Permanent address: University of Picardie, 80.000 Amiens, France.

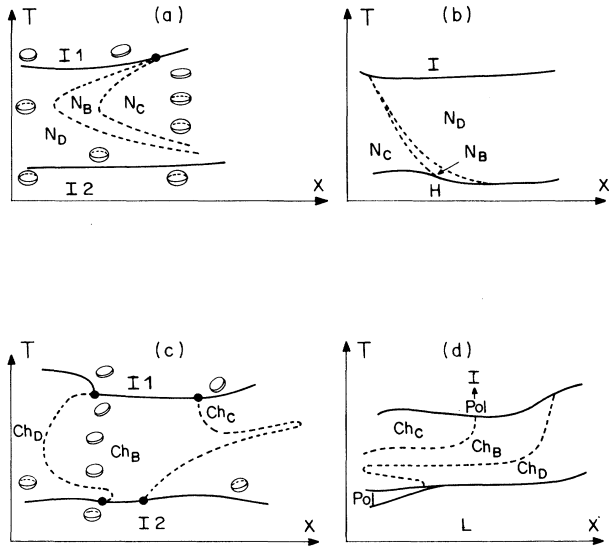

FIG. 1. Experimental temperature-concentration phase diagrams shown schematically. (a) and (b) Lyotropic nematic systems from Refs. [2] and [5]. (c) and (d) Lyotropic cholesteric systems from Refs. [7] and [8]. Full and dashed lines are first- and second-order transition lines, respectively. Curved platelets and flattened spheres in (a) and (c) symbolize the regions in which the biaxial and almost spherical micelles dominate. Pol, H, and L denote, respectively, a polyphase region, a hexagonal structure, and a lamellar structure. In all figures x represents the amphiphilic concentration of the mixture.

nature of the adjacent uniaxial nematic phase (N_D or N_C). In the chiral cholesteric variants [6–8] shown in Figs. 1(c) and 1(d) and found, for example, in potassium laurate/decanol/water ferrofluid [6], one has two three-phase points, instead of one four-phase point on the upper isotropic-nematic transition line, and two additional three-phase points appear on the transition line limiting the low-temperature structure, which can be isotropic [6], hexagonal [7], or lamellar [8]. Large polyphasic regions appear above and below the uniaxial Ch-C, Ch-D and biaxial (Ch-B) cholesteric phases [6,7].

The aim of the present work is to give a phenomenological description of the phase diagrams of Fig. 1, stressing the crucial influence of the shape modification of the molecular aggregates on the topology of the diagrams. The paper is organized as follows. In Sec. II, we show that the current model used for biaxial nematic systems, which was initially proposed for a fluid of rodlike and platelike molecules [9–12], applies only to the close vicinity of the high-temperature isotropic-nematic transitions line, but is insufficient to account for the behavior of the transition lines far from the preceding region, and for the existence of the reentrant isotropic phase and singular points observed at low temperatures. In Sec. III we establish that a full description of the nematic and cholesteric regions requires the introduction of an additional noncritical order parameter, which expresses the continuous change in the micellar shape when the temperature is lowered, and produces a *topological metamorphosis* [13,14] of the current two-component order-parameter phase diagrams [10,12]. In a preliminary report [15] the basic features of this specific nonlinear transformation, which has the effect of restructuring the preceding diagrams inducing a symmetric folding of the existing phases and singularities, were briefly described.

The theoretical description of the remaining areas of the experimental phase diagram, namely of the lamellar and hexagonal structures, which imply *topological transitions* [16] in the form of the molecular aggregates, will not be considered in the present paper.

II. THE C_{3v} MODEL

A. Macroscopic symmetry of the phases

From x-ray and neutron diffraction measurements [17,18], the N_C and N_D uniaxial nematic phases have been first analyzed to be, respectively, made of prolate and oblate micellar aggregates dispersed in water, the biaxial phase N_B being produced by a simple change of the micellar shape, assumed to transform from a flat disk (N_D) or an elongated cylinder (N_C) to a biaxial ellipsoid (N_B). Further careful measurements on lyotropic nematic phases [19,20] and lyotropic cholesteric phases [6] have revealed the following more subtle scheme. (1) In the three nematic phases, it was shown that within a large interval of temperatures and concentrations the micelles *mainly preserve their biaxial symmetry* and have, on average, the form of curved platelets of dimensions $\simeq 1 \times 2 \times 3$ (e.g., $\simeq 26$ Å$\times$ 55 Å$\times$ 85 Å). The differentiation between the phases was actually shown to be the macroscopic consequence of *different orientational spatial fluctuations of the platelets.* (2) One has a continuous decrease of the micellar shape anisotropy and orientational order when the temperature is lowered from approximately the middle of the nematic region to the Iso 2 phase [20–22]. The change of the micellar aggregates from curved platelets to *flattened sphere* shapes is clearly apparent when approaching the Iso 2 phase.

According to the first-mentioned fact, the micelles are orthorhombic objects with three distinct axes, but due to their spatial and thermal fluctuations the resulting macroscopic symmetries of the phases are determined by the probability distribution of orientation of the axes, which require *two directions* for their description corresponding to headless vectors denoted $\overleftrightarrow{n}$ and $\overleftrightarrow{m}$. Associating these two directions with the Euler angles (β,γ) and α, respectively, the actual probability distribution $P(\overleftrightarrow{n}, \overleftrightarrow{m})$ should be represented in a space of dimension larger than 3, in which the macroscopic symmetry of the phases would not clearly appear. Figure 2 shows the isotropic and nematic configurations in terms of the probability distribution $P(\beta, \gamma) = \int P(\overleftrightarrow{n}, \overleftrightarrow{m})\, d\alpha$ of *the longest orthorhombic axis to be oriented in the direction*

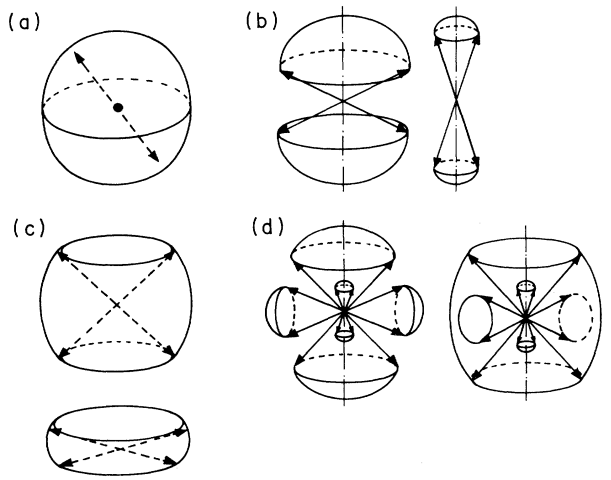

FIG. 2. Probability distribution $P(\overleftrightarrow{n})$ of the longest of the orthorhombic axes indicated by a double arrow, to be oriented in a given direction $\overleftrightarrow{n}$, in the (a) isotropic, (b) N_c, (c)N_D, and (d) N_B phases. In (b) and (c) the two figures symbolize the evolution from the isotropiclike to the cylindrical-like (b) and discoticlike (c) configurations of $P(\overleftrightarrow{n})$. In (d) two possible representations of $P(\overleftrightarrow{n})$ are given which possess, respectively, three maxima (left figure) and three minima (right figure). They illustrate the intermediate character of the N_B configurational symmetry with respect to the N_c and N_D symmetries. (b) and (c) can be equivalently replaced by revolution ellipsoids (prolate and oblate), and (d) by an ellipsoid with three different axes.

$\overleftrightarrow{n}$. Thus, if the probability is constant in all directions of the probability distribution space, one obtains the spherical distribution of Fig. 2(a) corresponding to the isotropic phase. If $P(\overleftrightarrow{n})$ is maximum along *one direction* or *within a plane* one gets, respectively, the N_C and N_D distributions which are given in Figs. 2(b) and 2(c). When $P(\overleftrightarrow{n})$ displays three simultaneous extrema (maxima or minima) in perpendicular directions as shown in Fig. 2(d), the N_B phase is stabilized.

From Fig. 2 one can see that, when assuming the z direction for the infinite-fold axis in the N_C phase, one will have, for a full rotational symmetry O(3) of the isotropic phase, the following point-group symmetries for the nematic phases: $D^{(z)}_{\infty h}$ [where z is the direction of the maximum of $P(\overleftrightarrow{n})$ for the N_C phase and is the direction of the minimum of $P(\overleftrightarrow{n})$ in the N_D phase] and D_{2h} (N_B). Starting from the chiral cholesteric isotropic phase, with symmetry SO(3), one has the corresponding lyotropic cholesteric point groups: $D^{(z)}_{\infty}$ (Ch-C and Ch-D) and D_2 (Ch-B). Let us note that the representation of $P(\overleftrightarrow{n})$ used in Fig. 2 is well adapted to the microscopic configuration of the micelles as one has for the N_C and N_D phases a cylindrical and a discotic shape for $P(\overleftrightarrow{n})$, respectively, but it is not unique. One may also use, instead of Figs. 2(b) and 2(c), prolate and oblate shapes which correspond to the same $D_{\infty h}$ symmetries for the phases and for the probability distribution of the micellar orientations. Along the same line, one may use an ellipsoidal representation of the biaxial probability distribution instead of Fig. 2(d).

B. Symmetry of the order parameter

The order parameters representing the orientational ordering of an isotropic medium transform as the irreducible representations (IR's) of the group $G_O = O(3)$ [or $G_O = SO(3)$ for a system of chiral molecules]. Following the current description of the nematic ordering from the isotropic state [23,24], which assumes only one direction which is sensed experimentally (the director), the probability density describing the orientation of the particles depends on the position vector $\vec{r}$ and on the direction $\overleftrightarrow{n}$. It can be written under the general form

$$\rho(\vec{r}, \overleftrightarrow{n}) = \sum_{\ell,m} \rho_{\ell m}(\vec{r})\, Y_{\ell m}(\overleftrightarrow{n}).$$

The $Y_{\ell m}$ are spherical harmonics of even index ℓ, and for a given ℓ, the coefficients $\rho_{\ell m}$ form a spherical tensor transforming as an IR of G_O, i.e., as the order parameter components. Phase transition in nematic systems are characterized by a tensor of rank 2 ($\ell = 2$). Actually any traceless second-rank tensor can be used even when assuming a biaxial nematic phase as, following the description of Freiser [9] and Alben [10–12], the average of a molecular property of biaxial symmetry can be represented by the following second-rank molecular tensor:

$$\overleftrightarrow{Q}_{nm} = \overleftarrow{n}\,\overrightarrow{n} - \overleftarrow{m}\,\overrightarrow{m},$$

where the headless vectors $\overleftrightarrow{n}$ and $\overleftrightarrow{m}$ are taken, respectively, along the longest axis of the molecules and along the perpendicular to their planes. $\overleftrightarrow{Q}_{nm}$ has *five* independent components which span a *five-dimensional irreducible representation* of O(3) [or SO(3)]. If one takes the average of $\overleftrightarrow{Q}_{nm}$ over the molecular orientations, the corresponding average tensor $\langle \overleftrightarrow{Q}_{nm} \rangle$ reflecting the macroscopic symmetries of the stable states can be written as

$$\langle \overleftrightarrow{Q}_{nm} \rangle = RTR^*,$$

where R is a unitary rotation matrix around $\overleftrightarrow{n}$ or $\overleftrightarrow{m}$, and T is a diagonal traceless matrix which fixes a reference configuration. The diagonal elements of T are the eigenvalues of $\langle \overleftrightarrow{Q}_{nm} \rangle$: $-\frac{1}{2}(\eta_1 + \sqrt{3}\,\eta_2)$, $-\frac{1}{2}(\eta_1 - \sqrt{3}\,\eta_2)$, η_1, where η_1 and η_2 constitute *the effective order-parameter components.* In other words, the three other components of the five-dimensional order parameter associated with the isotropic-to-biaxial nematic transition are "Goldstone" variables which do not influence the order-

ing of the micelles, but only the critical behavior of the system at the transition, as was noted in another framework by Lubensky and Priest [25,26].

In the effective two-dimensional order-parameter space, one can write in polar coordinates $\eta_1 = r\cos\theta$, $\eta_2 = r\sin\theta$, where r and θ have, respectively, the meaning of the overall deviation from isotropy and the deviation of a configuration from uniaxial symmetry. It should be emphasized that in the lyotropic systems under consideration, the preceding deviations must be understood in terms of the probability distribution $P(\overleftrightarrow{n}, \overleftrightarrow{m})$, namely for the spatial fluctuations of the platelets. This can be viewed by the fact that η_1 and η_2 have the symmetry of the spontaneous strain components:

$$\eta_1 \simeq \frac{1}{\sqrt{6}}\,(2\,\epsilon_{zz} - \epsilon_{xx} - \epsilon_{yy}) \quad \text{and} \tag{1}$$

$$\eta_2 \simeq \frac{1}{\sqrt{2}}\,(\epsilon_{xx} - \epsilon_{yy})$$

which express the orthorhombic deformation of an isotropic state ($\eta_1 = \eta_2 = 0$). Thus the uniaxial phases are obtained when two eigenvalues of the second rank tensor $\langle \overleftrightarrow{Q}_{nm} \rangle$ are equal (which gives, for example, $\eta_1 \neq 0, \eta_2 = 0$), the infinite-fold axis being along the third eigenvector. The biaxial symmetry is realized when the eigenvalues are unequal ($\eta_1 \neq \eta_2 \neq 0$).

From Eq. (1) one can see that η_1 and η_2 span a *two-dimensional irreducible representation* of a subgroup of O(3), as, for example, any of the cubic crystallographic groups [27]. Besides, the set of distinct matrices of this irreducible representation is isomorphous to an irreducible subgroup of O(2), composed by 2×2 orthogonal matrices acting on the "vector" representation (η_1,η_2), which constitute the *image-group* of G_O [28]. The generating matrices of this image group are

$$\frac{1}{2}\begin{pmatrix} -1 & -\sqrt{3} \\ \sqrt{3} & -1 \end{pmatrix} \text{ and } \begin{pmatrix} 1 & 0 \\ 0 & -1 \end{pmatrix}.$$

They correspond to the orthogonal matrices of the point-group C_{3v}. Accordingly the phase diagrams associated with the effective order parameter (η_1, η_2) will be *entirely* determined by the image symmetry C_{3v} [28,29].

C. Phase diagrams associated with the image C_{3v}

The basic polynomials which remain invariant under the transformation properties of the C_{3v} matrices (complete rational basis of invariants [29]) are

$$I_1 = \eta_1^2 + \eta_2^2 = r^2 \text{ and } I_2 = \eta_1^3 - 3\eta_1\eta_2^2 = r^3\cos 3\theta. \tag{2}$$

Thus the order-parameter (Landau) expansion can be written under the general form

$$F_1(I_1, I_2) = a_1 I_1 + b_1 I_2 + a_2 I_1^2 + c_{12} I_1 I_2 + a_3 I_1^3 + b_2 I_2^2 + \cdots. \tag{3}$$

Expansion (3) was discussed by a number of authors in connection with biaxial nematic systems [9–12,30] but also with ferroelastic transitions in cubic crystals [29,31]. Only some of the related phase diagrams, namely those for $a_2 > 0$, have been worked out. The procedure which allows a minimization of F_1 has been detailed in Refs. [29–31]. The results of the calculations and their relations with the experimental phase diagrams of Fig. 1 can be summarized as follows.

When F_1 is truncated at the *sixth degree* in r, which is the minimal degree necessary to obtain a biaxial phase [14], one gets a maximal number of *three* stable states. (i) Two *anti-isostructural* states with identical point group $D_{\infty h}$ (D_∞ for cholesterics) are obtained for the equilibrium condition $r \neq 0$, $\cos 3\theta = \pm 1$. They coincide with the uniaxial nematic phases N_D and N_C or with their cholesteric analogs Ch-D and Ch-C. (ii) One intermediate state of orthorhombic symmetry D_{2h} (D_2 for a biaxial cholesteric phase) is stabilized for $r \neq 0$, $\cos 3\theta \neq \pm 1$, corresponding to the N_B or Ch-B phase.

Figures 3 and 4 summarize the topological properties of the phase diagram associated with F_1 for different signs and values of the coefficients a_i, b_i, and c_{12}. Figures 3(a) and 3(b) show the diagrams currently assigned to a fluid of biaxial molecular subunits [10–12,30] in the two-

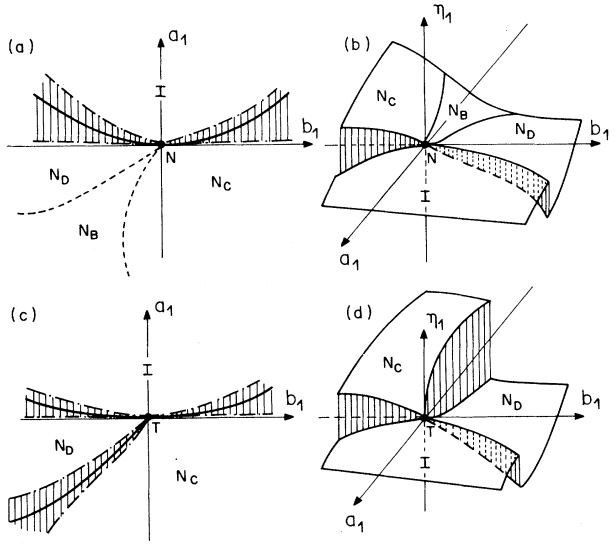

FIG. 3. Phase diagrams corresponding to F_1 (I_1, I_2) in the case $a_2 > 0$, $a_3 > 0$, and $\Delta = 4a_2\,b_2 - c_{12}^2 > 0$ [(a) and (b)], or $\Delta < 0$ [(c) and (d)]. Comments on the figures are given in the text. In (a) and (c), full, dashed, and dotted-dashed lines represent first-order, second-order, and limit of stability lines, respectively. Hatched surfaces are instability regions surrounding first-order transition lines. N is a four-phase (Landau) point and T is a triple point. In (b) and (d) the phases correspond to curved surfaces. The hatched surfaces represent the discontinuity of the order parameter on a first-order transition line.

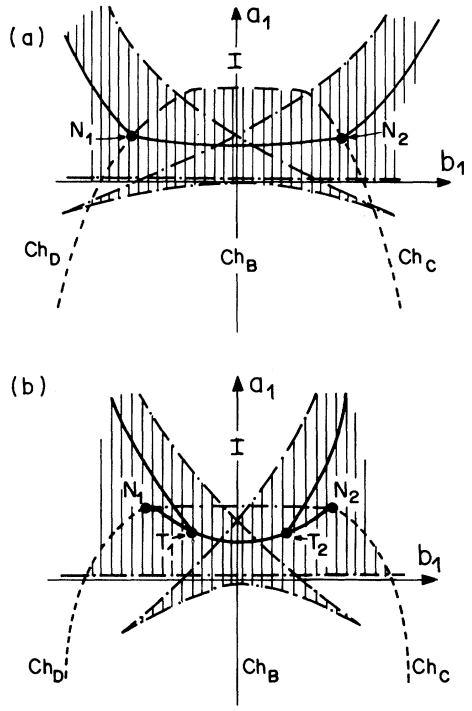

FIG. 4. Phase diagrams corresponding to F_1 (I_1, I_2) in the case $a_2 < 0$, $c_{12} = 0$, and (a) $0 < b_2 < a_3$, (b) $0 < a_3 < b_2$. Comments on the figures are given in the text. The notations and symbols for the phases and transition lines are the same as in Figs. 3(a) and 3(c). N_1 and N_2 are three-phase points in (a) and tricritical points in (b). T_1 and T_2 are triple points.

dimensional plane (a_1, b_1) and in the three-dimensional space (η_1, a_1, b_1). It indeed contains as in Figs. 1(a) and 1(b) a four-phase Landau point, at which merge two second-order transition lines [which become surfaces in Fig. 3(b)] separating the three nematic phases. The diagrams of Figs. 3(c) and 3(d) exhibit only the two uniaxial nematic phases separated by a first-order transition line: A direct first-order transition between the N_D and N_C phases has been actually reported [32,33] in the system sodium dodecyl-lauril sulfate–water–decanol, although this result remains to be confirmed by the order-parameter measurement across the transition, and by the temperature dependence of the observed phases.

The configurations shown in Fig. 3 are found when $a_2 > 0$. This coefficient appears to be related here to the chirality of the systems although no direct causal connection can be invoked in this respect. When a_2 becomes negative, one gets the phase diagrams represented in Fig. 4, which contain some features proper to cholesteric biaxial systems. Thus as in Figs. 1(c) and 1(d), Fig. 4(a) exhibits two three-phase points denoted N_1 and N_2. In the phase diagram of Fig. 4(b), N_1 and N_2 are *tricritical points*, and on the first-order transition line joining these points appear two additional *triple points* denoted T_1 and T_2.

Let us note that the first-order transition lines in Fig. 4 are surrounded by complex regions of phase coexistence, which reflect the large polyphasic regions found in lyotropic cholesteric phase diagrams [6,7]. These regions terminate within the nematic region by two unusual *metastability end points.*

D. Insufficiencies of the C_{3v} model for lyotropic systems

Despite a number of common features with the experimental diagrams of Fig. 1, the theoretical diagrams of Figs. 3 and 4 differ from the former in the following fundamental properties. (1) The lower reentrant isotropic phases cannot be obtained using expansion F_1, even when taking into account higher degree invariants. As shown in Fig. 5(a) for an eighth degree expansion of F_1, only reentrant uniaxial or cholesteric phases can be stabilized in this case. (2) The asymmetrical diverging cusp formed by the two second-order transition lines near the four-phase point [Fig. 3(a)] is an intrinsic feature of the C_{3v} model. This is illustrated in Fig. 5(b), which gives the general topology of the phase diagrams associated with F_1, in the plane of the invariants I_1 and I_2. Experimentally, one can see in Fig. 1(a) and Fig.

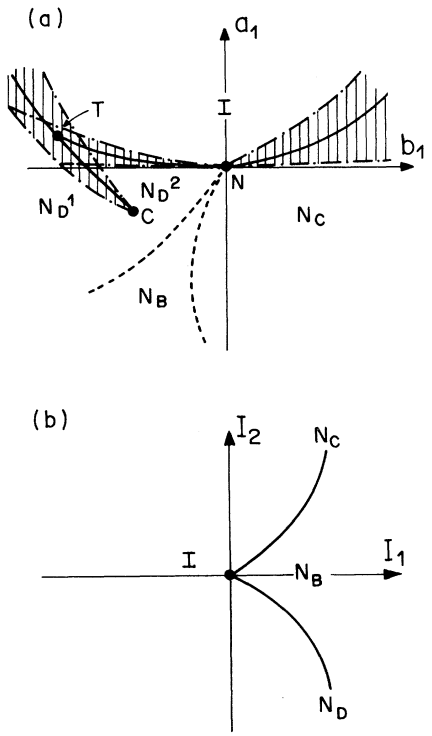

FIG. 5. (a) Phase diagram corresponding to F_1 (I_1, I_2) truncated to the *eighth* degree. A second nematic N_D^2 phase is stabilized, which is separated from N_D^1 by an isostructural transition line, ending at a critical point C. T is a triple point. The notations and symbols for the phases and transition lines are the same as in Figs. 3(a) and 3(c). (b) Phase diagram in the space of invariants (I_1, I_2), for the potential F_1 (I_1, I_2).

1(b) that the two lines possess the *same curvature* close to the Landau point. In Fig. 1(a) when decreasing the temperature, the two lines *diverge* towards lower concentrations, and, after a common inversion of their concavity, *converge again* versus large concentrations. This typical nonmonotonous regime cannot be obtained when assuming a *linear dependence* of the coefficients a_1 and b_1 on temperature and concentration. (3) Similar discrepancies are found for the cholesteric phase diagrams as the theoretical behaviors shown in Fig. 4 do not account for the nonmonotonous variation of the uniaxial-biaxial cholesteric transition lines, observed experimentally [6–8], or for the two additional three-phase points which appear on the first-order transition lines bounding the Iso 2, or hexagonal low-temperature structures [6–8].

Two experimental examples of temperature-concentration phase diagrams reported for distinct physical systems can help to understand the shortcomings of the C_{3v} model for interpretating the phase diagrams of lyotropic nematic and lyotropic cholesteric systems. In the mixed chromite compounds $Cr_{1-x}Ni_xCrO_4$ and $Fe_{1-x}Ni_xCrO_4$ [34], which also contain in their phase diagram a Landau point and are described by the same phenomenological approach as biaxial nematics, though the physical nature of the order parameter and the symmetries of the phases are different [31], the configuration of the transition lines in the vicinity of the Landau point (see Figs. 3 and 7 in Ref. [34]) is very close to the theoretical behavior shown in Fig. 3(a), with, in particular, a diverging cusp for the two second-order transition lines. In $Fe^{+2}Fe_x^{+3}Cr_{2-x}O_4$ [35], the transition lines merge at a three-phase point (Fig. 7 in Ref. [35]) with the same topology as the transition lines which merge at N_1 in Fig. 4(a).

Another instructive example is the temperature-concentration isostructural transition line found at the metal-semiconductor transition in the $Sm_{1-x}Gd_xS$ and $Sm_{1-x}Y_xS$ systems [36,37] which terminates at high and low temperatures by two critical points realizing a figure (Fig. 2 in Ref. [36]) very similar to the one formed by the second-order transition lines in the experimental diagram of Figs. 1(a) and 1(b). Here, the isostructural metal and insulator phases are the analogs of the anti-isostructural uniaxial nematic phases, the intermediate metastability region between the forward and reverse metal-insulator lines coinciding in Fig. 1 with the biaxial nematic phase. The phenomenological description of the phase diagram in the SmS family [38] assumes that the structural elements (ions) of the metal and semiconductor states are characterized by *different* dimensions and compressibilities, due to the difference of electronic configurations and corresponding Fermi surfaces.

From the preceding examples, one can infer that the model currently used for a fluid of biaxial particles applies successfully when the geometry of the particles (the atoms in mixed chromites) remains unchanged with decreasing temperature, but has to be completed when the form of the particles (e.g., the SmS ions) is modified as it has been observed experimentally for the micelles in lyotropic systems [6,19,21]. In the following section, we will show that when taking into account explicitly the observed changes in the *form* of the micellar aggregates with decreasing temperature, one obtains a *restructuring* of the theoretical phase diagrams of Figs. 3 and 4, which leads to a good agreement with the experimental diagrams of Fig. 1.

III. TOPOLOGICAL METAMORPHOSIS IN THE PHASE DIAGRAMS OF LYOTROPIC NEMATIC PHASES AND LYOTROPIC CHOLESTERIC PHASES

In this section we first expose a theoretical model of the isotropic-nematic transition, in which the modification in the shape of the micellar aggregates is shown to coincide with an additional *scalar* order parameter. Using the results of the catastrophe theory of restructuring of phase diagrams, we then demonstrate that the phase diagrams of lyotropic nematic and lyotropic cholesteric systems are drastically modified by this additional internal degree of freedom.

A. Phenomenological description of lyotropic nematic systems in which the micellar shape changes continuously

Let us first introduce the physical parameters which account both for the deformation of the micelles and for their orientation in space, in biaxial nematic systems. In real space, the orthorhombic deformation of a spherical micellar aggregate can be described by the strain-tensor $\hat{\epsilon}$. If the micellar volume is assumed to be *constant*, $\hat{\epsilon}$ is a traceless tensor, as $\epsilon_{xx} + \epsilon_{yy} + \epsilon_{zz} = 0$, and its *five* independent components can be written in spherical coordinates

$$\eta_0 = -\frac{\sqrt{3}}{2}(\epsilon_{xx} + \epsilon_{yy}),\ \eta_1 = -(\epsilon_{xz} + i\,\epsilon_{yz}),$$
$$\eta_2 = \frac{1}{2}(\epsilon_{xx} - \epsilon_{yy}) + i\,\epsilon_{xy},\ \eta_{-1} = -\eta_1^*,\ \eta_{-2} = \eta_2^*. \tag{4}$$

After diagonalization of $\hat{\epsilon}$ in the proper system of micellar axes, the preceding components become

$$\eta_0^d = -\frac{\sqrt{3}}{2}(\epsilon_{xx}^d + \epsilon_{yy}^d),$$
$$\eta_1^d = \eta_{-1}^d = 0,$$
$$\eta_2^d = \frac{1}{2}(\epsilon_{xx}^d - \epsilon_{yy}^d) = \eta_{-2}^d .$$

Using the same notation in real space as in the probability distribution space described in Sec. IIB, one can pose

$$\eta_0^d = r_a \cos\theta_a ,$$

$$\eta_2^d = \frac{1}{\sqrt{2}} r_a \sin\theta_a \quad \left(0 \leq \theta_a \leq \frac{\pi}{3}\right),$$

where r_a and θ_a are, respectively, the meaning of the deviation of the micellar form from a sphere (r_a=0) and from a revolution ellipsoid ($\theta_a = 0$).

Each couple of values of (r_a,θ_a) corresponds to a given micellar shape. The micelles which possess the same shape but different orientations in space can be obtained from a reference orientation in which the proper system of micellar axes coincides with the axes of a fixed frame, by application of the rotation $R(\alpha,\beta,\gamma)$, where α, β, and γ are the Euler angles, to the diagonalized components $(\eta_0^d, \eta_{\pm1}^d, \eta_{\pm2}^d)$. Accordingly the five components (η_i) are functions of the *five* variables (r_a,θ_a) *and* (α,β,γ).

Let us now develop a theoretical model of the isotropic-nematic transition, which *includes* a possible deformation of the micelles. The space of the order parameter associated with the preceding transition identifies to the space of the probability distribution $\wp(\hat{\epsilon}) = \wp(r_a,\theta_a,\alpha,\beta,\gamma)$, where $\wp(\hat{\epsilon})d\hat{\epsilon}$ is the probability for a micelle to exhibit the deformation (r_a,θ_a), *and* to be oriented in directions defined by the angular variables (α,β,γ). The number of micelles per unit volume with a given deformation is $n(\hat{\epsilon}) = n_0\,\wp(\hat{\epsilon})$, where n_0 is the number of micelles per unit volume. In order to determine the relevant transition order parameter one can select among the set of physical nth degree tensors $T^{[n]}$ associated with $\wp(\hat{\epsilon})$ the ones which coincide with the observed structural symmetries. The $T^{[n]}$ tensors are defined as the average of the nth products $(\eta_i)^{n_i}$ $(i = \pm 2, \pm 1, 0)$:

$$T^{[n]} = \int \wp(\hat{\epsilon}) \prod_{i=1}^{5} (\eta_i)^{n_i}\, d\hat{\epsilon}, \tag{5}$$

where $[n]$ denotes the indices $(n_1,n_2,\ldots,n_5)$, $n_i = 0,1,\ldots,\infty$, and $n = \sum_i n_i$.

Each *reducible* tensor $T^{[n]}$ decomposes into irreducible tensors $\pi^{(p,s,t)}$ of rank $p+2s+3t$ which transform as the irreducible representation of rank $2p$ of SO(3). The $4p+1$ components of $\pi^{(p,s,t)}$ can be written as the averages

$$\pi_m^{(p,s,t)} = \langle [I_1(\eta_i)]^s [I_2(\eta_i)]^t \omega_m^{(p)}(\eta_i)\rangle, \tag{6}$$

where $m = -2P,\ldots,2P$. The $4p+1$ functions $\omega_m^{(p)}(\eta_i)$ are the p-degree polynomials of the order-parameter components (η_i) which transform as the spherical harmonics Y_m^{2p}. $I_1(\eta_i) = \eta_0^2 + 2\eta_1\eta_{-1} + 2\eta_2\eta_{-2}$ and $I_2(\eta_i) = \eta_0^3 + 3\eta_0(\eta_1\eta_{-1} - 2\eta_2\eta_{-2}) + 3\frac{\sqrt{6}}{2}(\eta_2\eta_{-1}^2 + \eta_1\eta_{-2}^2)$. The components $\pi_m^{(p,s,t)}$ as given by Eq. (6) form the so-called *moments* of the distribution $\wp(\hat{\epsilon})$ [39]. In the current description of the isotropic-nematic transition, only the moments $\pi_m^{(1,0,0)}$ corresponding to the second-rank irreducible tensor $\overleftrightarrow{Q}$ are considered. One can see from Eq. (6) that in this case the $\pi_m^{(1,0,0)}$ moments identify to the *averages* of the η_i. Using the system of variables $(r_a,\theta_a,\alpha,\beta,\gamma)$, one has $I_1(\eta_i) = r_a^2$, $I_2(\eta_i) = r_a^3 \cos 3\theta_a$.

Partial integration of $\wp(\hat{\epsilon})$ leads to the probability distribution defined in Sec. II A, which describes the orientational distribution of the micelles (Fig. 2):

$$\wp(\overleftrightarrow{n},\overleftrightarrow{m}) = \wp(\alpha,\beta,\gamma) = \int \wp(r_a,\theta_a,\alpha,\beta,\gamma) r_a^4 dr_a d\theta_a. \tag{7}$$

In order to express the *shape modification* of the micelles, one has to take into account the additional *scalar moment* $\pi^{(0,1,0)}$ which is defined as

$$\pi^{(0,1,0)} = \tau = \langle I_1(\eta_i)\rangle = \langle r_a^2\rangle = \int r_a^6 S(r_a,\theta_a) dr_a d\theta_a. \tag{8}$$

where

$$S(r_a,\theta_a) = \int \wp(r_a,\theta_a,\alpha,\beta,\gamma)\, \sin\beta\, d\alpha\, d\beta\, d\gamma \tag{9}$$

is the probability of a spherical micelle to undergo the deformation (r_a,θ_a). In summary, taking into account *both* the scalar order parameter τ *and* the second-rank tensor order parameter $\overleftrightarrow{Q}$ provides a description of the ordering distributions of deformed micellar aggregates.

In the framework of the preceding approach, the more general thermodynamic potential which expresses the interactions within the micellar system can be written as the sum

$$F = F_0 + \sum_{P=1}^{n} F^{(P)}$$

in which $F^{(P)}$ accounts for the interaction energy of P micelles, and F_0 is the internal energy of the micelles. F_0 is given by

$$F_0 = n_0 \int \phi_0(\hat{\epsilon})\, \wp(\hat{\epsilon})\, d\hat{\epsilon},$$

where $\phi_0(\hat{\epsilon})$ is the free energy of an isolated micelle:

$$\phi_0(\hat{\epsilon}) = a_{10} I_1(\hat{\epsilon}) + a_{01} I_2(\hat{\epsilon}) + \cdots + a_{st} I_1^s(\hat{\epsilon}) I_2^t(\hat{\epsilon}) + \cdots.$$

It yields

$$F_0 = n_0 [a_{10}\,\tau + a_{01}\,\pi^{(0,0,1)} + \cdots + a_{st}\,\pi^{(0,s,t)} + \cdots].$$

Along the same line, $F^{(1)}$ is defined by

$$F^{(1)} = n_0^2 \int \phi_1(\hat{\epsilon}_1,\hat{\epsilon}_2)\, \wp(\hat{\epsilon}_1)\, \wp(\hat{\epsilon}_2)\, d\hat{\epsilon}_1\, d\hat{\epsilon}_2,$$

where the average interaction between two micelles is

$$\phi_1(\hat{\epsilon_1},\hat{\epsilon_2}) = \sum_{ni(i=1-5)} b_{\{ni\}}[I_1(\hat{\epsilon_1})]^{n_1}[I_2(\hat{\epsilon_1})]^{n_2} \times[I_1(\hat{\epsilon_2})]^{n_3}[I_2(\hat{\epsilon_2})]^{n_4}[I_3(\hat{\epsilon_1},\hat{\epsilon_2})]^{n_5}$$

and

$$F^{(1)} = n_0^2 \sum_{\substack{n_i=0 \\ I=1-5}}^{\infty} b_{\{n_i\}} \int [I_1(\hat{\epsilon_1})]^{n_1}[I_2(\hat{\epsilon_1})]^{n_2}[I_1(\hat{\epsilon_2})]^{n_3} \times[I_2(\hat{\epsilon_2})]^{n_4}[I_3(\hat{\epsilon_1},\hat{\epsilon_2})]^{n_5}\wp(\hat{\epsilon_1})\wp(\hat{\epsilon_2})d\,\hat{\epsilon_1}\,d\,\hat{\epsilon_2}$$

the invariant $I_3\ (\hat{\epsilon_1},\hat{\epsilon_2}) = \hat{\epsilon_1}\cdot\hat{\epsilon_2}$ expressing the quadrupole interaction of two micelles. For example, if $a_{10000} = 1$ and the other coefficients are zero, $F^{(1)} = n_0^2 \int I_1(\hat{\epsilon_1})\ \wp\ (\hat{\epsilon_1})\ \wp\ (\hat{\epsilon_2})\ d\ \hat{\epsilon_1}\ d\ \hat{\epsilon_2} = n_0^2\tau$. If $a_{00001} = 1$ and the other coefficients are zero, the quadrupole interaction gives the free-energy contribution $F^{(1)} = n_0^2 \int \hat{\epsilon_1}\cdot\hat{\epsilon_2}\ \wp\ (\hat{\epsilon_1})\ \wp\ (\hat{\epsilon_2})\ d\ \hat{\epsilon_1}\ d\ \hat{\epsilon_2} = n_0^2\ (\eta_0^2 + 2\eta_1^2 + 2\eta_2^2) = n_0^2\ r^2$, where the η_i are the spherical coordinates of Q deduced from Eq. (4) by replacing ε_{ij} by Q_{IJ}. It is obvious that when taking into account the contribution of all the $F^{(P)}$ terms to F, one obtains an expansion in powers of the moments $\pi^{(p,s,t)}$. When restricting to lowest degrees of the expansion and to the lowest rank tensors $p+2s+3t = 1$ $(p = 1, s = t = 0)$ and $p+2s+3t = 2$ $(p = 0, s = 1, t = 0)$, i.e., to $\overleftrightarrow{Q}$ and τ, one has

$$F = \tilde{\alpha}\ (n_0)\tau + \tilde{\beta}\ (n_0)\tau^2 + \tilde{\gamma}\ (n_0)r^2 + \tilde{\delta}\ (n_0)r^3\cos 3\theta + \tilde{\mu}\ (n_0)r^4 + \tilde{\nu}\ (n_0)r^6\cos^2 3\theta + \tilde{\lambda}\ (n_0)r^2\tau + \cdots, \quad (10)$$

where the coefficients $\tilde{\alpha}$, $\tilde{\beta}$, $\tilde{\gamma}$, $\tilde{\delta}$, $\tilde{\mu}$, $\tilde{\nu}$, $\tilde{\lambda}$, ... are polynomials of the number n_0. Let us emphasize that the form of F given by Eq. (10) differs only from the Landau expansion defined by Eq. (3), by the addition of the sucessive invariants $\tau,\tau^2,\ldots$ of the scalar order parameter τ.

In the preceding considerations, it has been assumed that the micellar volume remains constant within the considered phases. However, a change in the volume of the micellar aggregates may occur when their shape is modified (and it will be shown in the next section that this may be indeed the case in lyotropic nematic phases). A relative change in the volume of the micelles corresponds to a nonzero trace for the strain-tensor $\hat{\epsilon}$:

$$\mu_a = \epsilon_{xx} + \epsilon_{yy} + \epsilon_{zz} = \frac{\Delta V}{V}$$

and one has to add a *sixth component* μ_a to the five η_i defined by Eq. (4). The corresponding components of the tensors $\pi^{(p,s,t,u)}$ can be written

$$\pi_m^{(s,t,p,u)} = \langle [I_1(\eta_i)]^s [I_2(\eta_i)]^t [\mu_a\ (\eta_i)]^u \omega_m^{(p)}(\eta_i)\ \rangle.$$

The average increase in volume of the spheres being expressed by the *additional moment* $\mu = \pi^{(0,0,0,1)} = \langle\mu_a\rangle$. As μ_a is a totally symmetric quantity under the operations of O(3), only η_0 has to be modified in Eq. (4), i.e., $\eta_0 = \frac{1}{\sqrt{6}}\ (2\ \epsilon_{zz} - \epsilon_{xx} - \epsilon_{yy})$, although the order parameter dimensionality corresponding to the second-rank tensor becomes six instead of five. Let us note in this respect that as the invariants $I_1(\eta_i)$, $I_2(\eta_i)$, and $\mu_a\ (\eta_i)$ can be expressed as functions of the diagonalized strain-tensor components ϵ_{xx}^d, ϵ_{yy}^d, and ϵ_{zz}^d, they do not change under the permutation of the three axes x, y, and z, and thus they are also invariant under the permutation group of three objects, which is actually C_{3v}.

B. Restructuring of the phase diagrams in lyotropic nematic and lyotropic cholesteric systems

In connection with the experimental phase diagrams of Fig. 1, the additional scalar (noncritical) order parameter τ introduced above represents the distribution of the micellar shape at each temperature and concentration. It describes the continuous configurational change of the micellar population when the temperature is lowered, and its tendency to a more isotropic shape which portends the reentrant low-temperature isotropic phase. From experiment the number n of aggregates corresponding to a given deformation (r_a, θ_a) can be estimated, for a given concentration of micelles, from the average intermicellar distance in x-ray diffraction bands, the micellar aggregation number, and the molar concentration of each component of the lyotropic mixture [19]. The temperature at which the micelles undergo a crossover from a predominantly biaxial shape to a predominantly spheroidal shape can be assumed to coincide with the decrease of the birefrigence as a function of temperature observed in the nematic region [22,40].

The influence of τ on the phenomenological description of the phase diagrams of lyotropic systems can be understood in the framework of the catastrophe theory of restructuring of phase diagrams, developed by Arnold [13,41], in which it coincides with an extravariable of the nonrigid internal degrees of freedom of the system, which preserves the existing singularities and leads to their multiplication. As it is shown in [13] in the general case, if there exist in a system several noncritical, nonsymmetry breaking additional degrees of freedom (variables), (1) the macroscopic symmetry group of the system acts on the additional variables in a trivial way; (2) the free energy, as a function of the extravariables, has no additional singularities; i.e., it can be represented by a so-called Morse function, which is a nondegenerate quadratic form of the variables. Hence, the quadratic invariant should be modified in order to take into account the action of the macroscopic symmetry group on the whole set of variables, including the additional ones. More concretely, following the procedure given in Refs. [14] and [41], when the additional variable τ is taken into account in the C_{3v} model, it has the consequence: (1) that a new linear invariant $I_3 = \tau$ must be taken into account in the order-parameter expansion (2) to induce a *nonlinear* transfor-

mation of the *quadratic* invariant, of the form $I_1' = I_1 \pm \tau^2$, the cubic invariant I_3 being unaffected by this transformation. Let us show that the invariant basis

$$I_1' = r^2 + \tau^2, \quad I_2 = r^3 \cos 3\theta, \quad I_3 = \tau \tag{11}$$

is the one adapted to the phenomenological description of the experimental phase diagrams of Fig. 1. We will assume the following simple form for the thermodynamic potential:

$$F_2(I_1' I_2, I_3) = a_1 I_1' + a_2 I_1'^2 + b_1 I_2 + b_2 I_2^2 + c_1 I_3 + c_2 I_3^2 \tag{12}$$

noting that it is formally identical to the expansion F given by Eq. (10), and obtained from different premises. In particular, one has the same linear and quadratic invariants of the scalar τ in F_2 as in F. The mathematical procedure used to construct the phase diagrams associated with F_2 is described in the Appendix. It leads to the diagrams which are represented in Figs. 6, 7, and 8. The effect of the invariant I_3 is shown in the two-dimensional space (I_2, I_3) represented in Fig. 6(a), where one can see that it produces a *symmetric folding* of the diagram of Fig. 5(b) with the stabilization of the Iso 2

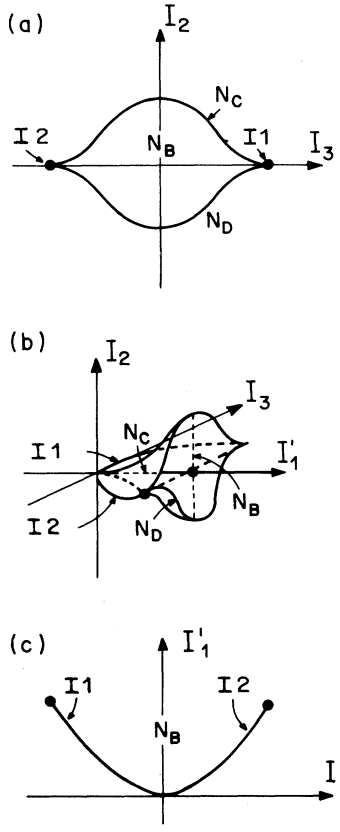

FIG. 6. Phase diagrams corresponding to F_2 (I_1', I_2, I_3) in two- and three-dimensional spaces of the invariants (I_1', I_2, I_3). Comments on the figures are given in the text.

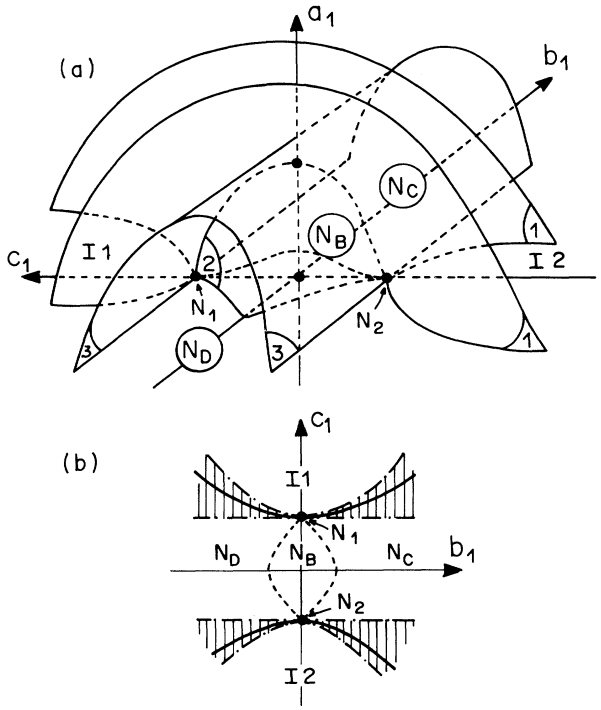

FIG. 7. Phase diagrams corresponding to F_2 (I_1', I_2, I_3) in spaces of the phenomenological coefficients. In (a) the transition and limit of stability *surfaces* are characterized by the numbers 1 (first-order), 2 (second-order), and 3 (limit of stability). In (b) the notations are the same as in Fig. 3(a). N_1 and N_2 are two four-phase (Landau) points.

phase. This *topological metamorphosis* of the region corresponding to the upper part of the phase diagram can be fully viewed in the three-dimensional invariant space (I_1', I_2, I_3) given in Fig. 6(b), which provides the topologies of the phases corresponding to lines (the isotropic phases), surfaces (the uniaxial phases), and volume (the biaxial phase). Figure 6(b) also reveals the neighborhoods between the phases, i.e., the possibility of going continuously, or through first-order transitions from one phase to another. One can verify in Fig. 6(c) that it is possible to go from one isotropic phase to the other *without transition*, as it has been shown experimentally [42] for very small concentrations of micellar aggregates.

Figure 7(a) represents the restructured phase diagram of Fig. 3(a) in the three-dimensional space of the phenomenological coefficients (a_1, b_1, c_1). It possesses a twofold symmetry of the singularities and phases with respect to the planes (a_1,c_1) and (a_1,b_1), as it can also be seen in the two-dimensional space (c_1,b_1) represented in Fig. 7(b). The diagram of Fig. 7(b) differs from the experimental diagrams of Figs. 1(a) and 1(b) by the fact that the second-order-transition lines are *symmetric* with respect to the c_1 and b_1 axes. Thus in order to obtain the *nonsymmetric* form reported experimentally, for the surface limited by the second-order transition lines, one has to perform a *linear* transformation in which the temperature T and the concentration x do not depend only

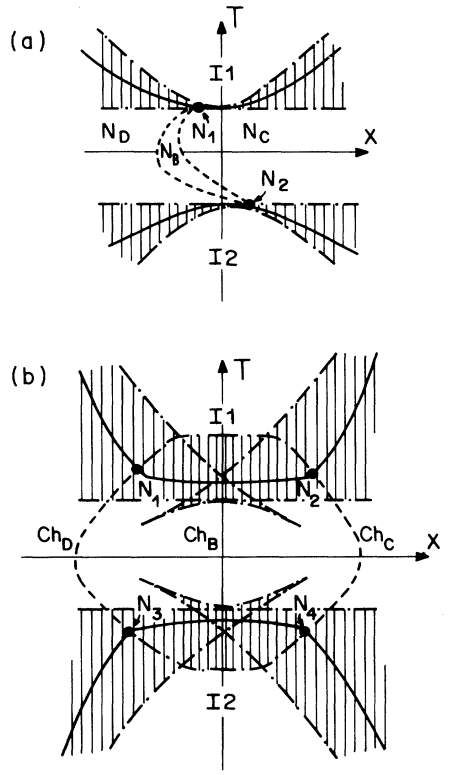

FIG. 8. Phase diagrams corresponding to F_2 (I_1', I_2, I_3) in the temperature concentration plane. Comments on the figures are given in the text. The notations are the same as in Fig. 3(a). In (a) N_1 and N_2 are four-phase points, whereas in (b) N_1, N_2, N_3, and N_4 are three-phase points.

on the coefficients a_1, b_1, and c_1, but also on *an adjusting constant*. This is related to the fact that we have chosen a symmetric form for the dependence of I_1' as a function of the extravariable τ. In the general case, this dependence is a quadratic form: $I_1' = r^2 + \tau^2 + \alpha\tau$, where α can be used as an adjusting constant for the curvature of the transition line. In the Appendix we show that one of the possible realizations of the adjusting constant is to coincide with the trace of the strain tensor $\epsilon_{xx} + \epsilon_{yy} + \epsilon_{zz}$. In other words, in order to obtain a theoretical temperature-concentration diagram consistent with the experimental observations, one may assume a relative change in the volume of the micelles.

When taking into account the preceding volume modification of the micelles, one gets by a linear transformation of b_1 and c_1 in functions of the temperature and concentration, the restructured phase diagrams shown in Figs. 8(a) and 8(b). One can verify that the essential features of the experimental diagrams are realized in these phase diagrams. Let us note that the second Landau point, denoted N_2 in Fig. 8(a), has been closely approached experimentally in a system in which the Iso 2 phase is replaced by a hexagonal phase [5]. The metastable hatched regions in Fig. 8(b) correspond to the polyphasic regions reported in all the lyotropic cholesteric systems [6–8].

The considered nonlinear transformation of the quadratic invariant $(I_1' = I_1 + \tau^2)$ is the only one acceptable for an interpretation of the phase diagrams of Fig. 1. For $I_1' = I_1 - \tau^2$ one can see in Figs. 9(a), 9(b), and 9(c) that the restructured diagram consists in two nematic regions separated by one isotropic phase, a situation that has not been observed experimentally. For $I_1' = I_1 + P^n(\tau)$, where $P^n(\tau)$ is a polynomial of degree $n = 3,4,\ldots$, one may have a tripling, quadrupling,... of the singularities, which is not adapted to the case under consideration, and is also very improbable from the point of view of the catastrophe theory. The preceding results correspond to a so-called *nontrivial* metamorphosis [41]. In the case of a *trivial* metamorphosis, which occurs when $I_1' = I_1$ or $I_1' = I_1 \pm \tau$, no multiplication of the singularities takes place.

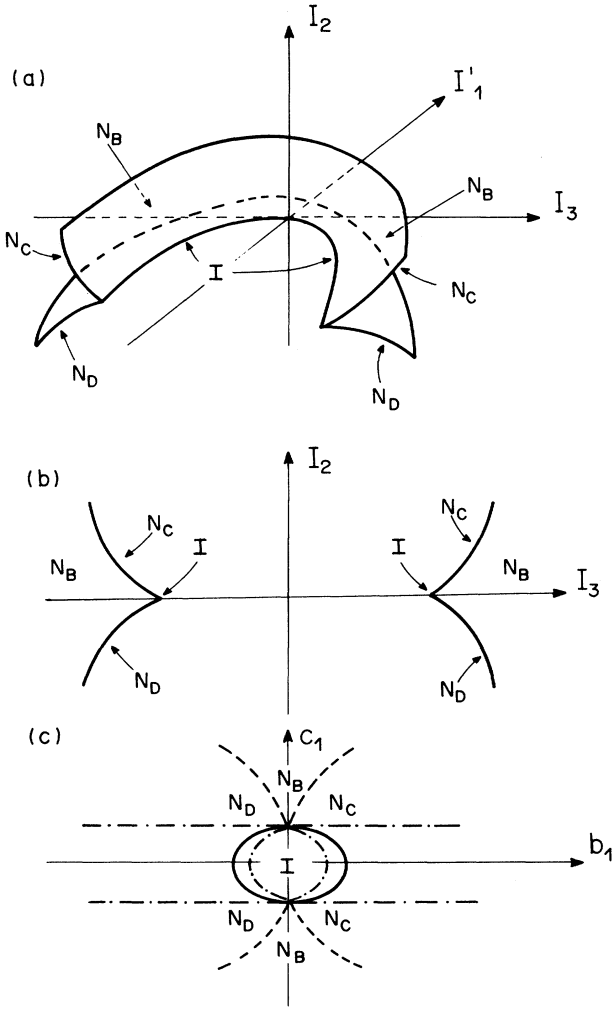

FIG. 9. Phase diagrams corresponding to F_2 (I_1', I_2, I_3) when $I_1' = I_1 - \tau^2$. Comments on the figures are given in the text. (a), (b), and (c) are the analog of Figs. 6(b), 6(a), and 7(b), respectively, obtained for $I_1' = I_1 + \tau^2$.

In summary, it has been shown that a phenomenological approach to the experimental phase diagrams of lyotropic nematic and lyotropic cholesteric liquids requires taking into account the modification of the micellar shape, *and possibly the variation of their volume.* The ordering and deformation processes are associated with two order parameters: a *six-dimensional* order parameter corresponding to a second-rank tensor with a *nonzero trace*, and a one-dimensional *scalar* order parameter. This latter parameter involves a restructuring of the theoretical phase diagrams proposed for a system of biaxial particles with unchanged shapes, a folding of the singular points, and a reentrance of the parent phase. It can be stressed that in the framework of the Landau theory of structural phase transitions [43], the role of nonsymmetry breaking order parameters is usually limited to a renormalization of the phenomenological coefficients in the (primary) order-parameter expansion, which has no effect on the basic features of the phase diagram. Here, the drastic topological changes induced by τ are related to the fact that this parameter expresses a modification of the *local* symmetry of the system, and an increase in the effective order parameter dimensionality. As a consequence, the number of *effective* phenomenological invariants forming the thermodynamic potential increases, resulting in additional phases and singularities *corresponding to preexisting symmetries* of the system. In this respect, it should be stressed that the description of the hexagonal or lamellar structures which replace, in a number of substances, the Iso 2 phase requires additional *symmetry breaking* order parameters [44].

ACKNOWLEDGMENTS

The authors are grateful to Fundação à Pesquisa do Estado de São Paulo for financial support.

APPENDIX

Let us recall the concepts of the theory of singularities [14] which have been used in the discussion of the potential F_2, given by Eq. (12). Denoting Ω a manifold of orbits in the space of the invariants $(I_1, I_2, \ldots, I_m)$ formed from the order parameter components (η_S), the Landau potentials form a family of functions defined on Ω:

$$F = F(\gamma_i, I_1, \ldots, I_m), \tag{A1}$$

where the γ_i are phenomenological coefficients. The equations of state of a system are given by

$$dF = \frac{\partial F}{\partial I_P}\frac{\partial I_P}{\partial \eta_S} d\eta_S = \frac{dF}{dI_P} dI_P = 0. \tag{A2}$$

$dI = (dI_1, dI_2, \ldots, dI_m)$ can be considered as a multidimensional vector tangent to the corresponding submanifold (stratum) of Ω. Equation (A2) expresses the property that the gradient $\frac{\partial F}{\partial \vec{I}}$ is perpendicular to the tangent vector. In a given stratum of Ω (a given phase) one has $\frac{\partial F}{\partial I_P} = b_{jP}(I_1, \ldots, I_m)\,\lambda_j$, where the b_{jP} $(j = 1, \ldots, k \leq m)$ form a normalized basis of the space orthogonal to $d\vec{I}$, and the λ_j the corresponding coordinate values. Separating in (A1) the terms linear in I_P, one can write (A2) under the form $\frac{\partial F}{\partial I_P} = \gamma_P + f_P(I_1, \ldots, I_m)$ or

$$\gamma_P = -f_P(I_1, \ldots, I_m) + b_{jP}\lambda_j. \tag{A3}$$

The stability of a given phase with respect to the thermodynamic fluctuations of the components (η_S), is defined by the positiveness of the second differential: $d^2F = \frac{\partial^2 F}{\partial I_P \partial I_k} dI_P dI_k + \frac{\partial F}{\partial I_P} d^2 I_P$, which can be written using (A3):

$$d^2F = df_P dI_P + \lambda_j\, b_{jP}\, d^2 I_P \geq 0. \tag{A4}$$

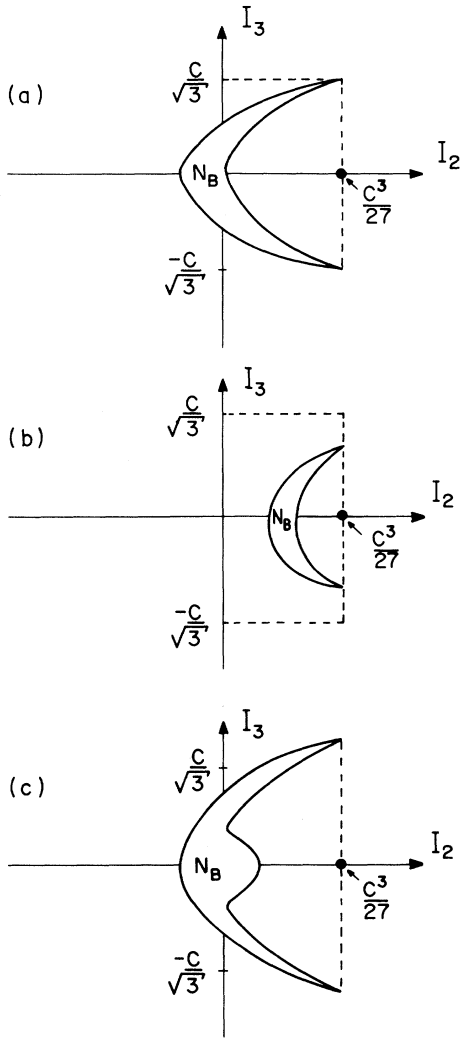

FIG. 10. Boundaries of the biaxial N_B phase given by Eq. (A5) for the following respective values of the trace t and of the constant $a_0 = I_1'$: (a) $a_0 = 0$, (b) $0 < a_0 < \frac{t^2}{3}$, (c) $a_0 < 0$. For $a_0 > \frac{t^2}{3}$ the biaxial phase is unstable.

Equation (A4) allows us to distinguish the boundaries of the phases which may be stable due to the symmetry of the system. To find the singularities of the phase diagram, one can use a potential F which has no singularity in functions of the I_P. Among the infinite number of such functions, the simplest (canonical) one, which accounts for the existing singularities, is the quadratic form of the I_P:

$$F = \sum_{P=1}^{m} (\gamma_P \, I_P \, + \, \tfrac{1}{2} \, a_P \, I_P^2).$$

Setting $a_P = 1$ for all the P, the equation of state (A3) takes the form

$$\gamma_P = -I_P + \lambda_j \, b_{jP}.$$

It is easy to show that the phase boundaries, corresponding to an equality in (A4), are given either by the conditions $\lambda_j = 0$ or by the degeneration of the matrix $M_{PS} = \| \frac{\partial \gamma_P}{\partial \eta_S} \|$ where $\eta_S = \eta_1, \ldots, \eta_k, \lambda_{k+1}, \ldots, \lambda_m$. In the space of the phenomenological coefficients γ_i the curve of hypersurfaces associated with $\lambda_j = 0$ has the same form as the stratum boundary on Ω. The degeneration of the M_{PS} matrix corresponds to an envelope of the family of vectors perpendicular to a given stratum on Ω. As the (η_S) are all different in the lowest symmetric phase, the M_{PS} matrix is not degenerate and the corresponding equation of state is $\frac{\partial F}{\partial I_P} = 0$, i.e., $\gamma_P = - I_P$. Let us use this latter property to show the specific form of the phase boundaries of the biaxial nematic phase N_B, as described by the thermodynamic potential F_2 (I_1', I_2, I_3), in which for simplicity we set $a_2 = b_2 = c_2 = \frac{1}{2}$. Thus the equation of state of the biaxial phase is given by $a_1 = - I_1'$, $b_1 = - I_2$, $c_1 = - I_3$. So that, up to the sign, a phase diagram in the space (I_1', I_2, I_3) is represented equivalently in the space of the coefficients (a_1, b_1, c_1). Writing the invariants under the form $I_1' = X_1 \, X_2 + X_2 \, X_3 + X_3 \, X_1 + \tau^2$, $I_2 = X_1 \, X_2 \, X_3$, and $I_3 = \tau$, where X_1, X_2, and X_3 are the eigenvalues of the second rank strain tensor with a nonzero trace: $X_1 + X_2 + X_3 = t$, the boundaries of the biaxial phase are defined by the conditions $\cos \theta = \pm 1$, or equivalently by $X_1 = X_2 \neq X_3$. Thus $X_3 = t - 2X_1$, and $I_1' = - 3X_1^2 + 2tX_1 + \tau^2$; $I_2 = - 2X_1^3 + tX_1^2$. In order to visualize a two-dimensional section of the three-dimensional phase diagrams (I_1', I_2, I_3), let us assume $I_1' = a_0$, where a_0 is a constant. The corresponding boundaries of the biaxial phase in the space (I_2, I_3) or (b_1, c_1) are given by

$$I_2 = -2X_1^3 + CX_1^2 = - b_1,$$

$$I_3 = \pm (-a_0 - 3X_1^2 + 2CX_1)^{\frac{1}{2}} = -c_1. \qquad \text{(A5)}$$

The different forms of the boundaries of the biaxial phase corresponding to different values of a_0 and t are shown in Figs. 10(a), 10(b), and 10(c). One can see from these figures, and from Eq. (A5), that the specific form reported experimentally for the biaxial phase boundaries, can be obtained for nonzero values of the trace t, i.e., when the volume of the micelles does *not* remain constant across the phase diagram.

[1] P.G. de Gennes, *The Physics of Liquid Crystals* (Clarendon, Oxford, 1975).
[2] J. Charvolin, Nuovo Cimento **3D**, 3 (1984).
[3] M.C. Holmes and J. Charvolin, J. Phys. Chem. **88**, 810 (1984).
[4] L.J. Yu and A. Saupe, Phys. Rev. Lett. **45**, 1000 (1980).
[5] E.A. Oliveira, L. Liebert, and A.M. Figueiredo Neto, Liq. Cryst. **5**, 1669 (1989).
[6] M.C. Valente Lopes and A.M. Figueiredo Neto, Phys. Rev. A **38**, 1101 (1988).
[7] M.E. Marcondes Helene and A.M. Figueiredo Neto, Mol. Cryst. Liq. Cryst. **162B**, 127 (1988).
[8] A.M. Figueiredo Neto and M.E. Marcondes Helene, J. Phys. Chem. **91**, 1466 (1987).
[9] M.J. Freiser, Phys. Rev. Lett. **24**, 1041 (1970).
[10] R. Alben, Phys. Rev. Lett. **30**, 778 (1973).
[11] R. Alben, J. Chem. Phys. **59**, 4299 (1973).
[12] C.S. Shih and R. Alben, J. Chem. Phys. **57**, 3055 (1972).
[13] V.I. Arnol'd, Commun. Pure Appl. Math. **29**, 557 (1976).
[14] E.I. Kut'in, V.L. Lorman, and S.V. Pavlov, Usp. Fiz. Nauk. **161**, 109 (1991) [Sov. Phys. Usp. **34**, 497 (1991)].
[15] P. Toledano and A.M. Figueiredo Neto, Phys. Rev. Lett. **73**, 2216 (1994).
[16] I.M. Lifshitz, Zh. Eksp. Teor. Fiz. **38**, 1569 (1960) [Sov. Phys. JETP **11**, 130 (1960)].
[17] J. Charvolin, A.M. Levelut, and E. Samulski, J. Phys. (Paris) Lett. **40**, L587 (1979).
[18] Y. Hendrikx, J. Charvolin, M. Rawiso, L. Liebert, and M.C. Holmes, J. Phys. Chem. **87**, 3991 (1983).
[19] Y. Galerne, A.M. Figueiredo Neto, and L. Liebert, J. Chem. Phys. **87**, 1851 (1987).
[20] A.M. Figueiredo Neto, Y. Galerne, A.M. Levelut, and L. Liebert, J. Phys. (Paris) Lett. **46**, L499 (1985).
[21] A.M. Figueiredo Neto, Y. Galerne, and L. Liebert, Liq. Cryst. **10**, 751 (1991).
[22] Y. Galerne, A.M. Figueiredo Neto, and L. Liebert, Phys. Rev. A **31**, 4047 (1985).
[23] P.G. de Gennes, Phys. Lett. A **30**, 454 (1969).
[24] W. Maier and A. Saupe, Z. Naturforsch. **14a**, 882 (1959).
[25] T.C. Lubensky and R. Priest, Phys. Lett. **48A**, 103 (1974).
[26] R.G. Priest and T.C. Lubensky, Phys. Rev. **B13**, 4159 (1976).
[27] V. Janovec, V. Dvořak, and J. Peltzelt, Czech. J. Phys. **B25**, 1362 (1975).
[28] Yu. M. Gufan, Fiz. Tverd. Tela (Leningrad) **13**, 225 (1971) [Sov. Phys. Solid State **13**, 175 (1971)].
[29] Yu. M. Gufan, *Structural Phase Transitions* (Nauka, Moscow, 1982).
[30] P.B. Vigman, A.I. Larkin, and V.M. Filev, Zh. Eksp.

Teor. Fiz. **68**, 1883 (1975) [Sov. Phys. JETP **41**, 944 (1975)].
[31] V.R. Sakhnenko and V.M. Talanov, Fiz. Tverd. Tela (Leningrad) **21**, 2435 (1979) [Sov. Phys. Solid State **21**, 1401 (1980)].
[32] L.Q. Amaral, Liq. Cryst. **7**, 877 (1990).
[33] L.Q. Amaral and M.E. Marcondes Helene, J. Phys. Chem. **92**, 6094 (1988).
[34] M. Kataoka and J. Kanamori, J. Phys. Soc. Jpn. **32**, 113 (1972).
[35] H.J. Levinstein, M. Robbins, and C. Capio, MRS Bull. **7**, 27 (1972).
[36] I.L. Aptekar' and E.Yu. Tonkov, Fiz. Tverd. Tela (Leningrad) **21**, 189 (1979) [Sov. Phys. Solid State **21**, 110 (1979)].
[37] I.L. Aptekar', V.J. Rashchupkin, and E.Yu. Tonkov, Fiz. Tverd. Tela (Leningrad) **21**, 1566 (1979) [Sov. Phys. Solid State **21**, 897 (1979)].
[38] Yu.M. Gufan and V.L. Lorman, Fiz. Tverd. Tela (Leningrad) **25**, 1038 (1983) [Sov. Phys. Solid State **25**, 598 (1983)].
[39] T.W. Anderson, *An Introduction to Multivariate Statistical Analysis* (John Wiley, New York, 1958).
[40] Y. Galerne and J.P. Marcerou, Phys. Rev. Lett. **51**, 2109 (1983).
[41] V.I. Arnol'd, A.N. Varchenko, and S.M. Gusein-Zade, *Singularities of Differential Maps* (Birkhauser, Boston, 1985 and 1988), Vols. 1 and 2.
[42] A.M. Figueiredo Neto, Y. Galerne, and L. Liebert, J. Phys. Chem. **89**, 3937 (1985).
[43] J.C. Toledano and P. Toledano, *The Landau Theory of Phase Transitions* (World Scientific, Singapore, 1987), Chap. 3.
[44] B. Mettout *et al.* (unpublished).